Case Studies in Thermal Engineering 36 (2022) 102190

Contents lists available at ScienceDirect

Case Studies in Thermal Engineering

journal homepage: www.elsevier.com/locate/csite

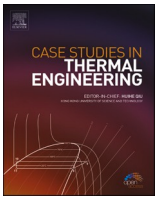

Thermal cooling process by nanofluid flowing near stagnating point of expanding surface under induced magnetism force: A computational case study

Faisal Shahzad [a], Wasim Jamshed [a], Amjad Ali Pasha [b], Rabia Safdar [c], Md. Mottahir Alam [d], Misbah Arshad [e], Syed M. Hussain [f], Muhammad Bilal Hafeez [g,*], Marek Krawczuk [g]

[a] Department of Mathematics, Capital University of Science and Technology (CUST), Islamabad, 44000, Pakistan
[b] Aerospace Engineering Department, King Abdulaziz University, Jeddah, 21589, Saudi Arabia
[c] Department of Mathematics, Lahore College for Women University, 54000, Lahore, Pakistan
[d] Department of Electrical and Computer Engineering, King Abdulaziz University, Jeddah, 21589, Saudi Arabia
[e] Department of Mathematics, Comsats University Islamabad, Sahiwal Campus, Pakistan
[f] Department of Mathematics, Faculty of Science, Islamic University of Madinah, 42351, Saudi Arabia
[g] Gdansk University of Technology, Faculty of Mechanical Engineering and Ship Technology, Institute of Mechanics and Machine Design, Narutowicza 11/12, 80-233, Gdańsk, Poland

ARTICLE INFO

Keywords:
Stagnation point
Heat source
Induced magnetic field
Titanium alloy-Water
Entropy generation

ABSTRACT

This paper is dedicated to the exam of entropy age and research of the effect of mixing nanosolid additives over an extending sheet. In this review, Newtonian nanofluid version turned into researched at the actuated appealing field, heat radiation and variable heat conductivity results. With becoming modifications, the proven PDEs are moved into popular differential situations and paintings mathematically making use of a specific mathematical plan called the Keller box method (KBM). The ranges of different dimensionless parameters used in our study are volume fraction of nanoparticles $0.01 \leq \varphi \leq 0.04$, magnetic parameter $0.5 \leq \Lambda \leq 2$, thermal radiation $0.1 \leq Nr \leq 0.3$, heat source/sink parameter $0.5 \leq Q_0 \leq 2$, Prandtl number $5.7 \leq Pr \leq 6.2$, variable thermal conductivity $0.1 \leq \varepsilon \leq 0.3$, reciprocal magnetic Prandtl number $0.6 \leq \lambda^* \leq 1$, Brinkman number $5 \leq Br \leq 15$, Reynolds number $5 \leq R_e \leq 15$, which shows up during mathematical arrangement are shown as tables and charts.Positive modifications in heat radiation and heat conductivity affects increment the hotness pass coefficient of solar primarily based totally plane wings. Titanium alloy primarily based totally water (H_2O) are taken into consideration for our research. We will likewise alternate the grouping of nanoparticles to pay attention on their impact on numerous dynamic barriers of the framework. We can see that because the Reynolds range and Brinkman range increment, the entropy increments. The thermodynamic exhibition of Titanium alloy-water (Ti_6Al_4V–H_2O) nanofluid has been portrayed higher that of base nanofluid with comparable situations. Recorded hypothetical reproductions may be greater beneficial to similarly increase daylight primarily based totally nuclear strength frameworks.

* Corresponding author.
E-mail address: muhammad.bilal.hafeez@pg.edu.pl (M.B. Hafeez).

https://doi.org/10.1016/j.csite.2022.102190
Received 24 April 2022; Received in revised form 3 June 2022; Accepted 5 June 2022
Available online 22 June 2022

Nomenclature

A^*	stretching rate ratio parameter
B_1	magneticcomponents along x
B_2	magneticcomponents along y
B_r	Brinkman number
C_f	drag force
C_p	specific-heat $(Jkg^{-1}K^{-1})$
c	stretching rate
κ	thermal conductivity $(Wm^{-1}K^{-1})$
k^*	absorption coefficient
N_r	radiation parameter
N_G	dimensionless entropy generation
Nu_x	local Nusselt number
M	magnetic parameter
P_r	Prandtl number (ν/α)
q_r	radiative heat flux
q_w	wall heat flux
Q_0	heatsource/sink parameter
R_e	Reynolds number
u, v	velocity component in x, y direction (ms^{-1})
U_w	velocity of the stretching sheet
x, y	dimensional space coordinates (m)
¥	fluid temperature
$¥_w$	fluid temperature of the surface
$¥_\infty$	ambient temperature
φ	volume fraction of the nanoparticles
ρ	density Kgm^{-3}
σ^*	Stefan Boltzmann constant
ψ	stream function
ξ	independent similarity variable
θ	dimensionless temperature
$\wedge$	magnetic parameter
ε	Variable thermal conductivity parameter
μ	dynamic viscosity of the fluid $(kgm^{-1}s^{-1})$
ν	kinematic viscosity of the fluid (m^2s^{-1})
α	thermal diffusivity (m^2s^{-1})
λ^*	reciprocal magnetic Prandtl number

Subscripts

f	base fluid
nf	nanofluid
s	nanoparticles
Ti_6Al_4V	titanium alloy nanoparticles
H_2O	water base fluid

1. Background survey

Heat transfer could be a warm organizing teach that coordinating the gathering, utilize, alter, and exchange of control vitality between flexible plans. Warm move is isolated into diverse cycles, as warm conduction, warm convection, warm radiation, and vitality travel through arrange changes. Plans other than consider moving a wide degree of substance compounds (alter in climatic circumstances mass trade), either cold or bubbling, to achieve warm move. In any case, these procedures have different properties, they routinely happen meanwhile in an identical system. Warm exchange happens when the advancement of a tremendous stack of liquid (gas or liquid) passes on its drive into a fluid. All convective cycles moreover convey inadequate force to the course, too [1]. Heat move is maybe the really present-day connection. All through the advanced field, intensity ought to be added, deducted, or wiped out from the dispersing of one cooperation to another. On a fundamental level, the power scattered by a hot liquid is never comparable to the force procured by a crisp liquid as a result of the lack of typical force [2]. Application for heat move in modern creation the vast

majority of creation utilizes a particular cycle to move heat. Drying processes are types of intensity move. The modern purposes of intensity move liquids fluctuate, from basic, dry plan to cutting edge measured frameworks that fill numerous roles in the creation cycle. As there are numerous varieties in the plan and use of cycles in the use of power move fluids, the number of adventures that use this procedure is moreover gigantic [3]. Scaling down immensely impacts the progress of control exchangers and changes warm exchangers into more limited and more talented. The viability of the control exchanger marvelously impacts the common reasonability and victory of the atomic control structure. A small channel warm sink is another instrument in warm exchange change. The likely picks up of a colossal control move locale and the tall cohesiveness of a small channel warm sink make it an astoundingly accommodating control exchanger for the utilization of electronic cooling [4].

Nanofluid could be a liquid that incorporates nanometer-sized particles, recognized as nanoparticles. These fluid colloidal suspensions are stressed nanoparticles in key fluid. Nanoparticles utilized in Nano liquid are for the greatest component fabricated from metals, oxides, carbides or carbon nanotubes. Distinctive standard fluids have been utilized as a working fluid to move hotness to diverse cycles. As a working liquid, water is for the most part utilized since of its tall openness, however it isn't seen as a compelling warm transporter since of its nonappearance of warm conductivity. Non-trade fluids, for case, engine oil, ethylene glycol, and so on, are moreover utilized in a collection of utilizations, be that as it may tall consistency and harmful climate constrain the utilization of these blends in warm exchange forms [5]. A combination of ethylene glycol and water utilized in general as a vehicle coolant, the development of nanoparticle moves forward the engine cooling rate. Electronic cooling of joined circuit and chip circuits has extended as of late, predominant execution PCs with a most extraordinary constrain of 100–300w/cm2 [6]. The warm exchange of normal convection of Newtonian Nanofluid on the outside surface of the laminar constrain is inquired about in an exact way. It has been watched that the convection warm exchange of customary convection isn't fair depicted by the energetic Nano fluid of warm conductivity which abhorrence to the thickness show utilized appears apparent and accept a critical portion in warm exchange conduct [7]. The speculation of past what numerous would consider conceivable layer has appeared amazingly gigantic and has given stunning capacity to the appraisal of liquid equipment since the turn of the hundred a long time. One of the rule occupations of minor concept is the assessment of pulling bodies on the stream, for case dragging a level plate in a zero position, an all over, airfoil, plane body, or turbine edge [8]. Within the progressing outline, the hotness moves and stream of pseudo-plastic non-Newtonian Nano fluid over the entering surface was settled where there was imbuement and ingestion. By imbuement and non-combination plate, non-Newtonian Nano fluid appears superior hotness move execution appeared up contrastingly comparing to Newtonian Nano fluid. By the by, altering the kind of nanoparticles by and large impacts the warm exchange handle amid back [9].

The heat source was chosen to allow the most power to be used to unwind the glass in order to draw the fiber without causing high-quality weight or choppiness in the neck-down zone. An increasing heat supply will result in a fiber with a consistent width and high quality. To attract fibers, oxygen lamps, CO_2 lasers, obstacle radiators, and enrollment radiators were used. On the basis of fire, an oxyhydrogen light, yet a pristine wellspring of heat, meets choppiness. A CO_2 laser is an extremely expensive heat source that should be considered for large-scale strand accumulation. The maximum component applied hotness hotspots for fiber drawing are graphite-obstruction radiators and zirconia-enlistment radiators. A graphite-resistive thing within the graphite-competition radiator transmits the important heat [10]. Since graphite responds with oxygen at tall temperatures, an inactive climate (e.g., argon) is kept up with interior the radiator. The zirconia-enlistment radiator doesn't require an idle climate. The radiator climate really ought to be spotless to provide high-strength fibers. A zirconia-acceptance radiator, when fittingly arranged and utilized, has conveyed uncommonly high-strength long-length fibers (over 2.0 GPa) in distances of many kilometers. Warm source could be a significant component in manufactured combination for moving forward the reactivity of reactants. Common warming interaction might be organized into three frameworks: radiation, warm conduction, and convection [11]. These warming modes are for the most part moo beneficial, and unavoidably bring temperature slants into the reaction media. In this way it requires a few speculations to reach at an agreement state. Microwave and ultrasound made a difference warming methodology can conceivably vanquish these issues through totally startling calefaction forms. Wang's gathering declared a clear procedure to secure t-YVO_4 NPs utilizing a family microwave. The combination of adequate $Y(NO_3)_3$ and $NaVO_3$ course of action was kept in a refluxing system and a short time later it went through a 10-min microwave light in enveloping discuss. The particle estimate went from 5 to 18 nm as shown by different reaction pH. The tiniest NPs appeared up at pH 7. One more sort of conceivable oxidative impetuses, $CeVO_4$ NPs were made essentially [12].

The induced magnetic field creates it's proclaim engaging subject in the fluid; thusly, it could amend the primer engaging subject. Jha and Sani [13] showed semi-logical, mathematical and illustrative arrangements for MHD highlight convection course of an electrically completing and gooey incompressible liquid in an upward channel in view of symmetric warming in the proximity of impelled engaging subject. Kumar and Singh [14] tried the shaky MHD free convective flow past a semi-wearisome vertical divider through method of method for pondering the started engaging subject. In another related work, Singh et al. [15] showed mathematical relationship for the hydro attractive free convective dissemination in an upward direct in the proximity of impelled engaging subject. A remember on hydro attractive free convective flow in the closeness of impelled engaging subject has been accomplished through method of method for Ghosh et al. [16]. Lately, Sarveshanand and Singh [17] showed precise relationship for MHD free convective dissemination among vertical equal porous plates in the closeness of started engaging subject and saw that the started contemporary thickness will increment with increase in the engaging Prandtl number. Kwanza and Balakiyema [18] tried the hydromagnetic free convective dissemination past an endless vertical porous plate with incited engaging subject. Akbar et al. [19] thought about the exchange of nano-garbage for the peristaltic dissemination in an upside down channel with the impelled engaging subject. In another work, Akbar et al. [20] have investigated the impact of impelled engaging subject and intensity motion with the suspension of carbon nano-tubes for the peristaltic dissemination in a permeable channel. Lately, Sahin et al. [21] tried the impact of cross over engaging subject on faithful free convective intensity and mass change from a vast vertical isothermal penetrable plate with consistent pull thinking the achieved attractive subject, gooey/attractive dissipating and at first set up synthetic reaction. Jha and Aina [22] sensibly

thought about the tireless hydro attractive totally made customary convection course in a vertical microchannel designed through method of method for endless vertical equal plates in the closeness of impelled engaging subject. From the presence of mind perspective, the closeness of impelled engaging subject play an urgent component in the investigate and speculative considers of MHD course due to its utilize in several component and progressive wonders, for example in MHD electric control period, the magneto hydrodynamics can be applied for crushing the new plasma, the pace of boats is estimated through method of method for MHD dissemination meter wherein the activated voltage is comparative with the flow rate, geophysics, filtration of crude oil, glass manufacturing and so on. For more details see Refs. [23–30].

A stagnation factor in fluid dynamics can be an area in a flow discipline in which the liquid's pace is zero [31]. The suspicion that any parcel of a flow discipline mendacity alongside some obstacles contains not anything however stagnation appears to seem in all however the maximum amazing instances of liquid factors inside the body of the "No-slip condition"; the suspicion that any parcel of a flow discipline mendacity alongside some obstacles contains not anything however stagnation appears to seem in all however the maximum amazing instances of liquid factors inside the body of the "No-slip condition" (the deal with as to whether or not this suspicion displays fact or is essentially a systematic consolation has been a nonstop problem of speak approximately seeing that the guideline of thumb turned into to start with set up).The Bernoulli condition appears that the inactive weight is most elevated when the speed is zero and subsequently inactive weight is at its most extreme esteem at stagnation focuses: in this case inactive weight breaks even with stagnation weight [32]. The Bernoulli condition appropriate to incompressible stream appears that the stagnation weight is rise to the energetic weight furthermore inactive weight. Add up to weight is additionally rise to energetic weight also inactive weight so, in incompressible streams, stagnation weight is break even with to add up to weight [33]. (In compressible flows, stagnation weight is additionally broken even with to add up to weight giving the liquid toward the inside the stagnation point is brought to rest isentropic ally.) The stream particularly considers a lesson of stagnation focuses known as saddle focuses where the approaching streamlines gets avoided and coordinated outwards in a diverse heading; the streamline deflections are guided by separatrices. The stream within the area of the stagnation point or line can for the most part be depicted utilizing potential stream hypothesis, in spite of the fact that thick impacts cannot be ignored on the off chance that the stagnation point lies on a strong surface. When streams both of -dimensional or axisymmetric nature imping on every different orthogonally, a stagnation aircraft is formed, within which the up-coming streams are occupied digressively outwards; on this fashion at the stagnation aircraft, the speed thing standard to it aircraft is zero, whilst the extraneous thing is non-zero. Within the community of the stagnation factor, a community portrayal for the rate subject is also portrayed. Nanofluids fouling effect can furthermore increment or decrease the nucleation effervescent heat trade relying at the surface/liquid touch factor as illustrated through Phan et al., during which they regarded of their paintings that the most multiplied heat trade coefficient became gotten at barely factor near to both 90° or 0° [34]. aside from to creating use of nanofluid as a HTF in heat trade applications, which became the most motive within the back of the event of such class of liquid, it's miles moreover applied in, for case, sunscreen items [35], medication [36,37], diminishing homes contamination [38], appealing fixing [39], microbial gasoline cells [40], antibacterial action, and several different applications [41]. Information gotten from the Scopus database from 1995 to 2018 regarded an exponential increment within the quantity of knowledge with the word "nanofluids", however for the year 2018 that's maximum all told likelihood to manage with the up and coming facts to the positioning [42].

Thermal conductivity is a boundary of a material that is much of the time thought about customary. Anyway, a few check and theoretical thinks roughly have affirmed that heat conductivity is eagerly connected with temperature change [43–49]. Xiong and Guo [50] approved the homes on region amounts essentially founded absolutely on a one-layered summed up magneto-thermoelastic trouble. Wang et al. [51] tried summed up thermoelectricity with variable intensity material homes and found that variable intensity influences of variable temperature-laid out amounts fundamentally founded absolutely on a one-layered summed up magneto-thermoplastic trouble. Ezzat and El-Bary [52] reviewed the effects of variable warm conductivity in a trouble of a thermo-viscoelastic unfathomably extended void barrel and found that each one capacity with regards to the summed up hypothesis with a variable intensity conductivity explicitly range from the ones gotten for the summed up theory with a normal intensity conductivity. Abo-Dahab and Abbas [53] surveyed the quite comfortable daze trouble of summed up magneto-thermoelectricity and inferred that on the grounds that the variable intensity conductivity increases, the temperature increases, even as the winding and circle stresses decrease. These thinks around delineated that variable intensity conductivity out and out influences the material homes and the transport of region amounts [54]. Prompt changes of temperature can interestingly change the overall quite comfortable conductivity of a fabric. Hence, the impact of temperature-laid out factor heat conductivity should be thought about in data fiber-supported summed up thermoelectricity inconveniences persevered from warm pressure.A critical analysis of the nanofluids' potential and achievement on the heat transfer enhancement has been extensively studied by academicians and scientists, for instance, see Refs. [55–63].

Under the light of above mentioned literature there is still a room available for the researchers to examine the various aspects of heat transfer and velocity of the fluid flow. The novelty behind the present research is given below.

- Investigational consequences display that Titanium alloy-water has viscoelastic properties.
- By incorporating nanoparticles, the mechanical and heat reliable traits of titanium alloy-water (Ti_6Al_4V– H_2O) are incredibly improved, and titanium alloy-nanocomposite materials may have an extra full-size collection of uses.
- The cutting-edge paintings inspect computational research for actuated MHD warmth pass streaming of a nanoliquid throughout a prolonged sheet whilst thinking about variable heat conductivity, and gooey scattering using the single-phase model.
- The nanofluids pondered are created from titanium alloy nanomolecules and water as base fluids.
- The controlling PDEs framework is transformed into directly ODEs using the similitude method, and later on numeric preparations are created using the hearty Keller box method.

- ❖ The consequences of quickness and strength fields for long-term obstacles are outwardly proven and brought exhaustively using the MATLAB apparatus.
- ❖ Drag-energy and hotness transmission quotes are likewise assessed graphically and mathematically.

2. Modeling of the problem

The model under consideration depicts a moving flat surface with a rough extended velocity [64].

$$U_w(x,0) = cx. \tag{1}$$

In the incidence of an induced magnetic field $y = 0$ represents a robust two-dimensional static point flow about a linear stretch sheet. The fluid is moving in the direction of $y > 0$. It is estimated that the free flow velocity will be $U_e(x) = ax$ and the expansion velocity is $U_w(x) = cx$ such that $a, c > 0$ In addition, we assumed that H is the vector of the induced magnetic field, with $B_e(x) = B_o(x)$, where B_o is a uniform magnetic field upstream at a non-limited location. The parallel and normal components of B_1 and B_2 of the affected magnetic field H are added together. The normal component B_2 vanishes on the plane, while the parallel component B_1 becomes B_o. Fig. 1 depicts the problem's structure. The flow constitutive equation for viscous nanofluids with flexible thermal conductivity and radiative heat flux under the conventional boundary layer approximation is [62,65].

$$\partial_x \mathrm{u} + \partial_y v = 0, \tag{2}$$

$$\partial_x B_1 + \partial_y B_2 = 0, \tag{3}$$

$$u\partial_x u + v\partial_y u - \frac{\mu}{4\omega\rho_f}\left(B_1\partial_x B_1 + B_2\partial_y B_1\right) = \left(U_e d_x U_e - \frac{\mu B_e}{4\omega\rho_f} d_x B_e\right) + \left(\frac{\mu_{nf}}{\rho_{nf}}\right)\partial_{yy} u, \tag{4}$$

$$u\partial_x B_1 + v\partial_y B_1 - B_1\partial_x u - B_2\partial_y u = \mu_e \partial_{yy} B_1, \tag{5}$$

$$v_1\partial_x ¥ + v_2\partial_y ¥ = \frac{1}{(\rho C_p)_{nf}}\left[\partial_y\left(\kappa^*_{nf}(¥)\partial_y ¥\right)\right] - \frac{1}{(\rho C_p)_{nf}}\partial_y q_r + \frac{q}{(\rho C_p)_{nf}}(T - T_\infty) \tag{6}$$

The relevant boundary conditions are [65]:

$$\left.\begin{array}{l} u = U_w = cx,\ v = 0, ¥ = ¥_w, \partial_y B_1 = B_2 = 0,\ at\ y = 0, \\ u \to U_e = ax, ¥ \to ¥_\infty, B_1 = B_e(x)\ \to B_0\ x,\ as\ y \to \infty. \end{array}\right\} \tag{7}$$

2.1. Thermophysical characteristics of the nanofluid

Nanoparticle scattering in an aqueous liquid results in improved thermophysical characteristics. The parameters for nanofluid are listed in Table 1 [66–71].Where u, v, B_1 and B_2 are the $x-$ and $y-$ axis velocity and magnetic components, correspondingly. The density, dynamic viscosity, and thermal diffusivity of nanofluid are signified by ρ_{nf}, μ_{nf} and α_{nf} respectively. The temperature of the fluid is denoted by the letter T. Nanofluid's productive possessions could potentially be reflected in the possessions of the base fluid. Additionally, Ti_6Al_4V nanoparticles and solid nanoparticles volume fraction in the base fluid are detailed in Table 2. φ is the nanoparticle volumetric fraction coefficient. μ_f, ρ_f, $(C_p)_f$ and κ_f are dynamic viscosity, density, effective heat capacity and thermal conductivity of the basefluid consistently. The other properties ρ_s, $(C_p)_s$ and κ_s are the density, effective heat capacity and thermal

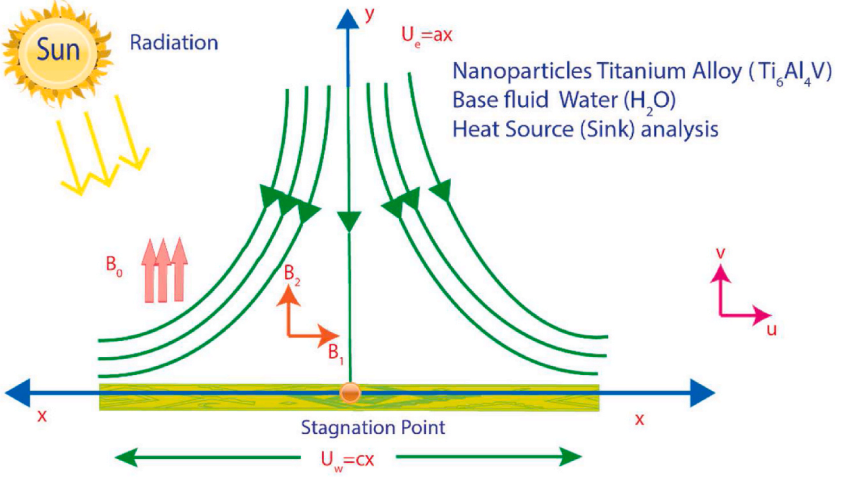

Fig. 1. Flow model schematic representation.

Table 1
Thermophysical features of nanofluid.

Properties	Nanofluid
Dynamic viscosity (μ)	$\mu_{nf} = \mu_f(1-\varphi)^{-2.5}$
Density (ρ)	$\rho_{nf} = (1-\varphi)\rho_f + \varphi\rho_s$
Heat capacity (ρC_p)	$(\rho C_p)_{nf} = (1-\varphi)(\rho C_p)_f + \varphi(\rho C_p)_s$
Thermal Conductivity (κ)	$\frac{\kappa_{nf}}{\kappa_f} = \left[\frac{(\kappa_s+(2)\kappa_f)-(2)\varphi(\kappa_f-\kappa_s)}{(\kappa_s+(2)\kappa_f)+\varphi(\kappa_f-\kappa_s)}\right]$

Table 2
Material characteristics of nanoparticles and basefluid at 293 K.

Thermophysical	$\rho(kg/m^3)$	$c_p(J/kgK)$	$k(W/mK)$
Water (H_2O)	997.1	4179	0.613
TitaniumAlloy (Ti_6Al_4V)	4420	526.3	6.7

conductivity of the nanoparticles, correspondingly. The variable thermal conductivity is indistinct as [72]:

$$\kappa^*_{nf}(¥) = k_{nf}\left[1+\varepsilon\frac{¥-¥_\infty}{¥_w-T_\infty}\right] \tag{8}$$

2.2. Features of basefluid and nanoparticles

The material parameters of the liquid water employed in this work, as well as other nanoparticles, are shown in Table 2 [63,73–75].

2.3. Rosseland approximations

By relating the Roseland approximation, one can mark [76].

$$q_r = -\frac{4\sigma^*}{3k^*}\frac{\partial ¥^4}{\partial y}, \tag{9}$$

Here, σ^* is the Stefan Boltzmann number and k^* is the absorption coefficient.

3. Model solution

The (BVP) equations (2)–(4) are moved using a similarity mathod, which converts the PDE into an ODE. Introduce the stream function, which takes the form

$$u = \frac{\partial \psi}{\partial y}, v = -\frac{\partial \psi}{\partial x}. \tag{10}$$

and similarity variables of the form

$$\left.\begin{gathered}\xi = \sqrt{\frac{b}{\nu_f}}y, B_1 = B_0 x G'(\xi), B_2 = -\sqrt{c\nu_f}G(\xi), \psi(x,y) = \sqrt{\nu_f b}xF(\xi), \\ \theta(\xi) = \frac{¥-¥_\infty}{¥_w-¥_\infty}.\end{gathered}\right\} \tag{11}$$

into equations (2)–(4). We get

$$\chi_a F''' - \chi_b\left[F'^2 - FF'' - A^{*2} - \Lambda\left(G'2 - GG'' - 1\right)\right] = 0, \tag{12}$$

$$\lambda^* G''' + FG'' - F''G = 0, \tag{13}$$

$$\theta''\left(1+\varepsilon\theta+\frac{1}{\chi_d}PrNr\right) + \varepsilon\theta'^2 + Pr\frac{\chi_c}{\chi_d}(F\theta' - F'\theta) + PrQ_0\frac{\chi_c}{\chi_d}\theta = 0, \tag{14}$$

with

$$\left.\begin{gathered}F(\xi) = G(\xi) = 0,\ F'(\xi) = 1,\ G''(\xi) = 0, \theta(\xi) = 1, at\ \xi = 0, \\ F'(\xi) \to A^*,\ G'(\xi) \to 1, \theta(\xi) \to 0\ as\ \xi \to \infty,\end{gathered}\right\} \tag{15}$$

where χ'$_i$s, $1 \le i \le 4$ in equations 12–14 show the subsequent thermophysical characteristics for the nanofluid

$$\left.\begin{aligned}\chi_a=(1-\varphi)^{-2.5},\chi_b=\left(1-\varphi+\varphi\frac{\rho_s}{\rho_f}\right),\chi_c=\left(1-\varphi+\varphi\frac{(\rho C_p)_s}{(\rho C_p)_f}\right)\\ \chi_d=\left(\frac{(k_s+2k_f)-2\varphi(k_f-k_s)}{(k_s+2k_f)+\varphi(k_f-k_s)}\right).\end{aligned}\right\} \tag{16}$$

Here, prime shows derivative with respect to ξ. Furthermore, Prandtl number Pr, stretching rate ratio parameter A^*, reciprocal magnetic Prandtl number λ^*, magnetic parameter Λ and the heat source/sink parameter Q_0 are secure as

$$\left.Pr=\frac{(\mu c_p)_f}{\kappa_f},\lambda^*=\frac{\mu_e}{\nu_f},\Lambda=\frac{\mu}{4\omega\rho_f}\left(\frac{B_0}{c}\right)^2,A^*=\frac{a}{c}.Q_0=\frac{q}{a(\rho C_p)_f}\right\} \tag{17}$$

3.1. Non-dimensional physical quantity of the model

The Skin friction coefficient C_f and Nusselt number Nu_x are the physical measures of which laeds the glow and can be defined as

$$C_f=\frac{\tau_w}{\rho(u_w)^2},\ Nu_x=-\frac{xq_w}{\kappa_f(T_w-T_\infty)}, \tag{18}$$

here q_w is heat flux at wall and τ_w is wall shear stress.We translate the overhead formulas into non-dimensional form using the similarity transformation (7).

$$Re_x^{1/2}C_f=\frac{-1}{(1-\varphi)^{2.5}}F''(0),\ Nu_xRe_x^{-1/2}=-\frac{\kappa_{nf}}{\kappa_f}\theta'(0) \tag{19}$$

where $Re_x=\frac{u_wx}{\nu_f}$ is local Reynolds number.

4. Entropy generation analysis

For the above-mentioned assumption, the entropy generation is [65]:

$$N_G=\frac{\kappa_{nf}}{T_w^2}\left[\left(\frac{\partial T}{\partial x}\right)^2+\left(\frac{\partial T}{\partial y}\right)^2\right]+\frac{\mu_{nf}}{T_w}\tau\cdot L. \tag{20}$$

The entropy equation in its dimensionless form is written as follows:

$$N_G=\frac{S_G}{S_{G_0}}=R_e\left[\frac{\kappa_{nf}}{\kappa_f}\varepsilon\left(\frac{\partial\theta}{\partial\xi}\right)^2+\frac{\mu_{nf}}{\mu_f}Br(F'')^2\right], \tag{21}$$

where dimensionless temperature variance is $\varepsilon=\frac{\Delta T}{T_w}$, Br is Brinkman number i.e. $Br=\frac{\rho_fC^3x^2}{\kappa_f\Delta T}$ and R_e is the Reynolds number.

5. Numerical procedure of the considered scheme

Nonlinear ODEs are being worked on (12-14) The Keller-box approach [77–79], which uses the algebraic programme MATLAB for distincit values of the corresponding parameters, is used in combination with the end point condition (15). The Keller-box scheme's step-by-step technique is as follows:

5.1. Conversion of ODEs

We get twitchy when we introduce new autonomous variables:

$Dp_1(x,\xi),Dp_2(x,\xi),Dp_3(x,\xi),Dp_4(x,\xi),\ Dp_5(x,\xi),\ Dp_6(x,\xi),\ Dp_7(x,\xi)$ and $Dp_8(x,\xi)$ with $Dp_1=F,\ Dp_2=F',\ Dp_3=F'',\ Dp_4=G,\ Dp_5=G',\ Dp_6=G'',\ Dp_7=\theta$ and $Dp_7=\theta'$. With this transformation, Eqs. 12–15shrink to thegivenODE form

$$\frac{dDp_1}{d\xi}=Dp_2, \tag{22}$$

$$\frac{dDp_2}{d\xi}=Dp_3, \tag{23}$$

$$\frac{dDp_4}{d\xi}=Dp_5, \tag{24}$$

$$\frac{dDp_5}{d\xi}=Dp_6, \tag{25}$$

$$\frac{dDp_7}{d\xi} = Dp_8, \tag{26}$$

$$A_1\frac{dDp_3}{d\xi} - A_2\left(Dp_2^2 - Dp_1Dp_3 - (A^*)^2 - \Lambda\left(Dp_5^2 - Dp_4Dp_5 - 1\right)\right) = 0, \tag{27}$$

$$\lambda^*\frac{dDp_6}{d\xi} + Dp_1Dp_6 - Dp_3Dp_4 = 0, \tag{28}$$

$$\left.\begin{aligned}\frac{dDp_8}{d\xi} + \varepsilon Dp_7\frac{dDp_8}{d\xi} + \frac{1}{\chi_d}PrNr\frac{dDp_8}{d\xi} + \varepsilon Dp_8^2 + Pr\frac{\chi_c}{\chi_d}Dp_1Dp_8 - Pr\frac{\chi_c}{\chi_d}Dp_2Dp_7 \\ + PrQ_0\frac{\chi_c}{\chi_d}Dp_7 = 0,\end{aligned}\right\} \tag{29}$$

$$\left.\begin{aligned}&Dp_1(0) = 0,\ Dp_2(0) = 0,\ Dp_4(0) = 0,\ Dp_6(0) = 1,\ Dp_7(0) = 1,\\ &Dp_2(\xi) \to A^*, \quad Dp_5(\xi) \to 1, \quad Dp_7(\xi) \to 0,\ as\ \xi \to \infty.\end{aligned}\right\} \tag{30}$$

5.2. Spatial discretization& difference equations

In the same way, domain discretization in the $x-$ plane is denoted. Net points are generated as a result of this web. $\xi_0 = 0, \xi_j = \xi_{j-1} + \delta L,\ j = 0, 1, 2, 3..., J, \xi_J = 1$ where, δL is the step-size. Relating central difference formulation at midpoint $\xi_{j-1/2}$

$$(Dp_1)(Dp_1)_j - (Dp_1)(Dp_1)_{j-1} = 1\Big/2*\delta L\Big((Dp_2)_j + (Dp_2)_{j-1}\Big), \tag{31}$$

$$(Dp_2)(Dp_2)_j - (Dp_2)(Dp_2)_{j-1} = 1\Big/2*\delta L\Big((Dp_3)_j + (Dp_3)_{j-1}\Big), \tag{32}$$

$$(Dp_4)(Dp_4)_j - (Dp_4)(Dp_4)_{j-1} = 1\Big/2*\delta L\Big((Dp_5)_j + (Dp_5)_{j-1}\Big), \tag{33}$$

$$(Dp_5)(Dp_5)_j - (Dp_5)(Dp_5)_{j-1} = 1\Big/2*\delta L\Big((Dp_6)_j + (Dp_6)_{j-1}\Big), \tag{34}$$

$$(Dp_7)(Dp_7)_j - (Dp_7)(Dp_7)_{j-1} = 1\Big/2^*\delta L\Big((Dp_8)_j + (Dp_8)_{j-1}\Big), \tag{35}$$

$$\left.\begin{aligned}&A_1\frac{\left((Dp_4)_j - (Dp_4)_{j-1}\right)}{\delta L} - A_2\left(\frac{Dp_2)Dp_2)\left(Dp_2)(Dp_2)_{j-1}\right)^2}{4} - \frac{\left((Dp_1)_j + (Dp_1)_{j-1}\right)}{2}\right.\\ &\left.\frac{\left((Dp_3)_j + (Dp_3)_{j-1}\right)}{2} - (A^*)^2 - \Lambda\left(\frac{Dp_5)Dp_5)\left(Dp_5)(Dp_5)_{j-1}\right)^2}{4} - \frac{\left((Dp_4)_j + (Dp_4)_{j-1}\right)}{2}\frac{\left((Dp_5)_j + (Dp_5)_{j-1}\right)}{2} - 1\right)\right) = 0\end{aligned}\right\}, \tag{36}$$

$$\left.\begin{aligned}&\lambda^*\frac{\left((Dp_4)_j - (Dp_4)_{j-1}\right)}{\delta L} + \frac{\left((Dp_1)_j + (Dp_1)_{j-1}\right)}{2}\frac{\left((Dp_6)_j + (Dp_6)_{j-1}\right)}{2}\\ &-\frac{\left((Dp_3)_j + (Dp_3)_{j-1}\right)}{2}\frac{\left((Dp_4)_j + (Dp_4)_{j-1}\right)}{2} = 0,\end{aligned}\right\}, \tag{37}$$

$$\left.\begin{aligned}&Dp_8)(Dp_8)_j - Dp_8)(Dp_8)_{j-1}\Big) + \varepsilon\frac{\left((Dp_7)_j + (Dp_7)_{j-1}\right)}{2}(Dp_8)_j - (Dp_8)_{j-1}\Big) + \frac{1}{\chi_d}PrNr\Big((Dp_8)_j - (Dp_8)_{j-1}\Big)\\ &+ \delta L\varepsilon\frac{Dp_8)Dp_8)\left(Dp_8)(Dp_8)_{j-1}\right)^2}{4}\\ &+\delta LPr\frac{\chi_c}{\chi_d}\frac{\left((Dp_1)_j + (Dp_1)_{j-1}\right)}{2}\frac{\left((Dp_8)_j + (Dp_8)_{j-1}\right)}{2}\\ &-\delta LPr\frac{\chi_c}{\chi_d}\frac{\left((Dp_2)_j + (Dp_2)_{j-1}\right)}{2}\frac{\left((Dp_7)_j + (Dp_7)_{j-1}\right)}{2} + PrQ_0\frac{\chi_c}{\chi_d}\frac{\left((Dp_7)_j + (Dp_7)_{j-1}\right)}{2} = 0,\end{aligned}\right\}, \tag{38}$$

5.3. method

The Newton's linearization technique is used to linearize Eqs. 31–38.

$$\left.\begin{array}{l}(Dp_1)_j^{n+1} = (Dp_1)_j^n + (\delta Dp_1)_j^n,\ (Dp_2)_j^{n+1} = (Dp_2)_j^n + (\delta Dp_2)_j^n,\\ (Dp_3)_j^{n+1} = (Dp_3)_j^n + (\delta Dp_3)_j^n,\ (Dp_4)_j^{n+1} = (Dp_4)_j^n + (\delta Dp_4)_j^n,\\ (Dp_5)_j^{n+1} = (Dp_5)_j^n + (\delta Dp_5)_j^n,\ (Dp_6)_j^{n+1} = (Dp_6)_j^n + (\delta Dp_6)_j^n,\\ (Dp_7)_j^{n+1} = (Dp_7)_j^n + (\delta Dp_7)_j^n,\ (Dp_8)_j^{n+1} = (Dp_8)_j^n + (\delta Dp_8)_j^n.\end{array}\right\} \tag{39}$$

The following sequence of equations can be generated by substituting the equations found in (31-38) and eliminating the power of to the square or more.

$$\Big(\delta Dp_1\Big)(\delta Dp_1)_j - \Big(\delta Dp_1\Big)(\delta Dp_1)_{j-1}\Big) - 1\Big/2{*}\delta L\Big((\delta Dp_2)_j + (\delta Dp_2)_{j-1}\Big) = (r_1)_j, \tag{40}$$

$$\delta Dp_2\Big)(\delta Dp_2)_j - \delta Dp_2\Big)(\delta Dp_2)_{j-1}\Big) - 1\Big/2{*}\delta L(\delta Dp_3)_j + (\delta Dp_3)_{j-1}\Big) = (r_2)_j, \tag{41}$$

$$\delta Dp_4\Big)(\delta Dp_4)_j - \delta Dp_4\Big)(\delta Dp_4)_{j-1}\Big) - 1\Big/2{*}\delta L(\delta Dp_5)_j + (\delta Dp_5)_{j-1}\Big) = (r_3)_j, \tag{42}$$

$$\delta Dp_5\Big)(\delta Dp_5)_j - \delta Dp_5\Big)(\delta Dp_5)_{j-1}\Big) - 1\Big/2{*}\delta L(\delta Dp_6)_j + (\delta Dp_6)_{j-1}\Big) = (r_4)_j, \tag{43}$$

$$\Big((\delta Dp_7)_j - (\delta Dp_7)_{j-1}\Big) - 1\Big/2 * \delta L\Big((\delta Dp_8)_j + (\delta Dp_8)_{j-1}\Big) = (r_5)_{j,} \tag{44}$$

$$\begin{array}{l}(\omega_1)_j(\delta Dp_3)_j + (\omega_2)_j(\delta Dp_3)_{j-1} + (\omega_3)_j(\delta Dp_2)_j + (\omega_4)_j(\delta Dp_2)_{j-1} +\\ (\omega_5)_j(\delta Dp_1)_j + (\omega_6)_j(\delta Dp_1)_{j-1} + (\omega_7)_j(\delta Dp_5)_j + (\omega_8)_j(\delta Dp_5)_{j-1} +\\ (\omega_9)_j(\delta Dp_4)_j + (\omega_{10})_j(\delta Dp_4)_{j-1} + (\omega_{11})_j(\delta Dp_6)_j + (\omega_{12})_j(\delta Dp_6)_{j-1} = (r_6)_j,\end{array} \tag{45}$$

$$\begin{array}{l}(\mu_1)_j(\delta Dp_6)_j + (\mu_2)_j(\delta Dp_6)_{j-1} + (\mu_3)_j(\delta Dp_4)_j + (\mu_4)_j(\delta Dp_4)_{j-1} + (\mu_5)_j(\delta Dp_6)_j\\ \qquad +(\mu_6)_j(\delta Dp_6)_{j-1} = (r_7)_j,\end{array} \tag{46}$$

$$\begin{array}{l}(\nu_1)_j(\delta Dp_1)_j + (\nu_2)_j(\delta Dp_1)_{j-1} + (\nu_3)_j(\delta Dp_2)_j + (\nu_4)_j(\delta Dp_2)_{j-1} + (\nu_5)_j(\delta Dp_7)_j\\ \qquad +(\nu_6)_j(\delta Dp_7)_{j-1} + (\nu_7)_j(\delta Dp_8)_j + (\nu_8)_j(\delta Dp_8)_{j-1} = (r_8)_j,\end{array} \tag{47}$$

where

$$\left.\begin{array}{l}\omega_1\Big)(\omega_1)_j = A_1 + \dfrac{A_2\delta L}{4}Dp_1\Big)(Dp_1)_j + Dp_1\Big)(Dp_1)_{j-1}\Big) = \omega_2\Big)(\omega_2)_j + 2A_1, \omega_3\Big)(\omega_3)_j = -\dfrac{A_2\delta L}{2}(Dp_2)_j + (Dp_2)_{j-1}\Big) = (\omega_4)_j,\\ \omega_5\Big)(\omega_5)_j = \dfrac{A_2\delta L}{4}Dp_3\Big)(Dp_3)_j + Dp_3\Big)(Dp_3)_{j-1}\Big) = \omega_6\Big)(\omega_6)_j, \omega_7\Big)(\omega_7)_j = -\dfrac{A_2\delta L\Lambda}{2}(Dp_5)_j + (Dp_5)_{j-1}\Big) = (\omega_8)_j,\\ \omega_9\Big)(\omega_9)_j = -\dfrac{A_2\delta L\Lambda}{4}Dp_6\Big)(Dp_6)_j + Dp_6\Big)(Dp_6)_{j-1}\Big) = \omega_{10}\Big)(\omega_{10})_j, \omega_{11}\Big)(\omega_{11})_j = -\dfrac{A_2\delta L\Lambda}{2}(Dp_4)_j + (Dp_4)_{j-1}\Big) = (\omega_{12})_j,\\ (r_6)_j = -A_1\dfrac{\Big((Dp_4)_j - (Dp_4)_{j-1}\Big)}{\delta L} + A_2\left(\dfrac{Dp_2\Big)Dp_2\Big)\Big(Dp_2\Big)(Dp_2)_{j-1}\Big)^2}{4} + \dfrac{\Big((Dp_1)_j + (Dp_1)_{j-1}\Big)}{2}\right.\\ \dfrac{\Big((Dp_3)_j + (Dp_3)_{j-1}\Big)}{2} - (A^*)^2 + \Lambda\left(\dfrac{Dp_5\Big)Dp_5\Big)\Big(Dp_5\Big)(Dp_5)_{j-1}\Big)^2}{4} + \dfrac{\Big((Dp_4)_j + (Dp_4)_{j-1}\Big)}{2}\right.\\ \left.\left.\dfrac{\Big((Dp_5)_j + (Dp_5)_{j-1}\Big)}{2} - 1\right)\right),\end{array}\right\} \tag{48}$$

$$\left.\begin{aligned}
&\mu_1\Big)(\mu_1)_j=\lambda^*+\frac{\delta L}{4}Dp_1\Big)(Dp_1)_j+Dp_1\Big)(Dp_1)_{j-1}\Big)=\mu_2\Big)(\mu_2)_j+2\lambda^*,\mu_3\Big)(\mu_3)_j=-\frac{\delta L}{4}(Dp_3)_j+(Dp_3)_{j-1}\Big)=(\mu_4)_j,\\
&\mu_5\Big)(\mu_5)_j=-\frac{\delta L}{4}Dp_4\Big)(Dp_4)_j+Dp_4\Big)(Dp_4)_{j-1}\Big)=\mu_6\Big)(\mu_6)_j,\mu_7\Big)(\mu_7)_j=\frac{\delta L}{4}(Dp_6)_j+(Dp_6)_{j-1}\Big)=(\mu_8)_j,\\
&(r_7)_j=\lambda^*\frac{\Big((Dp_4)_j-(Dp_4)_{j-1}\Big)}{\delta L}+\frac{\Big((Dp_1)_j+(Dp_1)_{j-1}\Big)}{2}\frac{\Big((Dp_6)_j+(Dp_6)_{j-1}\Big)}{2}-\frac{\Big((Dp_3)_j+(Dp_3)_{j-1}\Big)}{2}\frac{\Big((Dp_4)_j+(Dp_4)_{j-1}\Big)}{2},
\end{aligned}\right\}\tag{49}$$

$$\left.\begin{aligned}
&(\nu_1)_j=\delta L\frac{Pr\chi_c}{\chi_d}\frac{\Big((Dp_8)_j+(Dp_8)_{j-1}\Big)}{4}=(\nu_2)_j,\\
&(\nu_3)_j=-\delta L\frac{Pr\chi_c}{\chi_d}\frac{\Big((Dp_8)_j+(Dp_8)_{j-1}\Big)}{4}=(\nu_4)_j,\\
&(\nu_5)_j=\delta L\frac{Pr\chi_c}{\chi_d}\frac{\Big((Dp_2)_j+(Dp_2)_{j-1}\Big)}{4}+\varepsilon\frac{\Big((Dp_8)_j-(Dp_8)_{j-1}\Big)}{2}=(\nu_6)_j\\
&(\nu_7)_j=1+\frac{NrPr}{\chi_d}+\delta L\frac{Pr\chi_c}{\chi_d}\frac{\Big((Dp_1)_j+(Dp_1)_{j-1}\Big)}{4}+\varepsilon\frac{\Big((Dp_7)_j-(Dp_7)_{j-1}\Big)}{2}+\delta L\varepsilon\frac{\Big((Dp_8)_j-(Dp_8)_{j-1}\Big)}{2}+PrQ_0\frac{\chi_c}{\chi_d}\frac{\Big((Dp_7)_j-(Dp_7)_{j-1}\Big)}{2},\\
&(\nu_8)_j=-1-\frac{NrPr}{\chi_d}+\delta L\frac{Pr\chi_c}{\chi_d}\frac{\Big((Dp_1)_j+(Dp_1)_{j-1}\Big)}{4}+\varepsilon\frac{\Big((Dp_7)_j-(Dp_7)_{j-1}\Big)}{2}+\delta L\varepsilon\frac{\Big((Dv_8)_j-(Dv_8)_{j-1}\Big)}{2}+PrQ_0\frac{\chi_c}{\chi_d}\frac{\Big((Dp_7)_j-(Dp_7)_{j-1}\Big)}{2}\\
&r_8\Big)(r_8)_j=-Dp_8\Big)(Dp_8)_j-Dp_8\Big)(Dp_8)_{j-1}\Big)-\varepsilon\frac{\Big((Dp_7)_j+(Dp_7)_{j-1}\Big)}{2}(Dp_8)_j-(Dp_8)_{j-1}\Big)\\
&-\frac{1}{\chi_d}PrNr\left((Dp_8)_j-(Dp_8)_{j-1}\right)+\delta L\varepsilon\frac{Dp_8\Big)Dp_8\Big)\Big(Dp_8\Big)(Dp_8)_{j-1}\Big)^2}{4}+\delta LPr\frac{\chi_c}{\chi_d}\frac{\Big((Dp_1)_j+(Dp_1)_{j-1}\Big)}{2}\frac{\Big((Dp_8)_j+(Dp_8)_{j-1}\Big)}{2}\\
&+\delta LPr\frac{\chi_c}{\chi_d}\frac{\Big((Dp_2)_j+(Dp_2)_{j-1}\Big)}{2}\frac{\Big((Dp_7)_j+(Dp_7)_{j-1}\Big)}{2}-PrQ_0\frac{\chi_c}{\chi_d}\frac{\Big((Dp_7)_j-(Dp_7)_{j-1}\Big)}{2}.
\end{aligned}\right\}\tag{50}$$

5.4. Block tridiagonal structure

The linear system now has a block tridiagonal structure, which is denoted by

$$A\Delta=S,\tag{51}$$

where

$$A=\begin{bmatrix}
[L_1] & [N_1] & & & & & \\
 & [L_2] & [N_2] & & & & \\
 & & \ddots & & & & \\
 & & & \ddots & & & \\
 & & & & [M_{J-1}] & [L_{J-1}] & [N_{J-1}] \\
 & & & & & [M_J] & [L_J]
\end{bmatrix},\ \Delta=\begin{bmatrix}[\Delta_1]\\ \vdots\\ \vdots\\ \vdots\\ [\Delta_{J-1}]\\ [\Delta_J]\end{bmatrix}\text{ and }S=\begin{bmatrix}[S_1]\\ \vdots\\ \vdots\\ \vdots\\ [S_{J-1}]\\ [S_J]\end{bmatrix}.$$

where the elements defined in Eq. (51) are

$$[L_1]=\begin{bmatrix} 0 & 0 & 0 & 1 & 0 & 0 \\ -1/2*\delta L & 0 & 0 & 0 & 0 & 0 \\ -1 & 0 & -1/2*\delta L & 0 & -1/2*\delta L & 0 \\ 0 & -1 & 0 & 0 & 0 & -1/2*\delta L \\ (\omega_6)_1 & 0 & (\omega_8)_1 & (\omega_1)_1 & (\omega_7)_1 & 0 \\ 0 & (\nu_6)_1 & 0 & (\nu_1)_1 & 0 & (\nu_7)_1 \end{bmatrix},$$

$$[L_j]=\begin{bmatrix} -1/2*\delta L & 0 & 0 & 1 & 0 & 0 \\ -1 & -1/2*\delta L & 0 & 0 & 0 & 0 \\ 0 & -1 & 0 & 0 & -1/2*\delta L & 0 \\ 0 & 0 & -1 & 0 & 0 & -1/2*\delta L \\ (\omega_4)_j & (\omega_6)_j & 0 & (\omega_1)_j & (\omega_7)_j & 0 \\ (\nu_4)_j & 0 & (\nu_6)_j & (\nu_1)_j & 0 & (\nu_7)_j \end{bmatrix}, 2 \le j \le J$$

$$[M_j]=\begin{bmatrix} 0 & 0 & 0 & -1 & 0 & 0 \\ 0 & 0 & 0 & 0 & 0 & 0 \\ 0 & 0 & 0 & 0 & -1/2*\delta L & 0 \\ 0 & 0 & 0 & 0 & 0 & -1/2*\delta L \\ 0 & 0 & 0 & (\omega_2)_j & (\omega_8)_j & 0 \\ 0 & 0 & 0 & (\nu_2)_j & 0 & (\nu_8)_j \end{bmatrix}, 2 \le j \le J$$

$$[N_j]=\begin{bmatrix} -1/2*\delta L & 0 & 0 & 0 & 0 & 0 \\ 1 & -1/2*\delta L & 0 & 0 & 0 & 0 \\ 0 & 1 & 0 & 0 & 0 & 0 \\ 0 & 0 & 1 & 0 & 0 & 0 \\ (\omega_3)_j & (\omega_5)_j & 0 & 0 & 0 & 0 \\ (\nu_3)_j & 0 & (\nu_5)_j & 0 & 0 & 0 \end{bmatrix}, 1 \le j \le J-1.$$

Now we factorize A as

$$A = LU, \tag{51}$$

where

$$L=\begin{bmatrix} [\Gamma_1] & & & & \\ & [\Gamma_2] & & & \\ & & \ddots & & \\ & & \ddots & [\Gamma_{J-1}] & \\ & & & [M_J] & [\Gamma_J] \end{bmatrix}, U=\begin{bmatrix} [I] & [\alpha_1] & & & \\ & [I] & [\alpha_2] & & \\ & & \ddots & \ddots & \\ & & & [I] & [\alpha_{J-1}] \\ & & & & [I] \end{bmatrix},$$

where the total size of the block-triangle matrix A is $J \times J$, each block size of the supervector is 6×6, and $[I]$, $[\Gamma_i]$ and $[\alpha_i]$ are 6th-order matrices. is. Claim of LU decomposition algorithm for solving Δ. A mesh size of $\Delta h_j = 0.01$ is considered suitable for mathematical assessment and the result is gained with an error tolerance of 10^{-6}.

6. Code validation

The literatures [80,81]was compared to the available results to verify the results obtained. The consistency comparisons in the study are summarised in Table 3. However, the findings of this investigation were extremely accurate.

7. Results and discussion

The goal of this study is to determine the overall results of the thermal system in the presence of induced MHD nanofluid warps and

Table 3
Comparison of $-\theta'(0)$ with variation in Prandtl number, and taking $\varepsilon = 0$, $\varphi = 0$, $Q_0 = 0$ and.$A^* = 0$.

P_r	Ref. [80]	Ref. [81]	Present
0.72	0.8087612	0.8087618	0.8087618
1.0	1.0000000	1.0000000	1.0000000
3.0	1.9235743	1.9235742	1.9235742
7.0	3.0731467	3.0731465	3.0731465
10	3.7205543	3.7205542	3.7205542

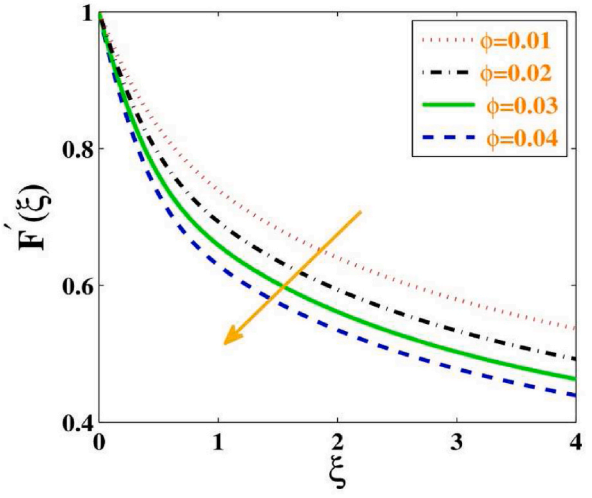

Fig. 2. Velocity variation versus φ.

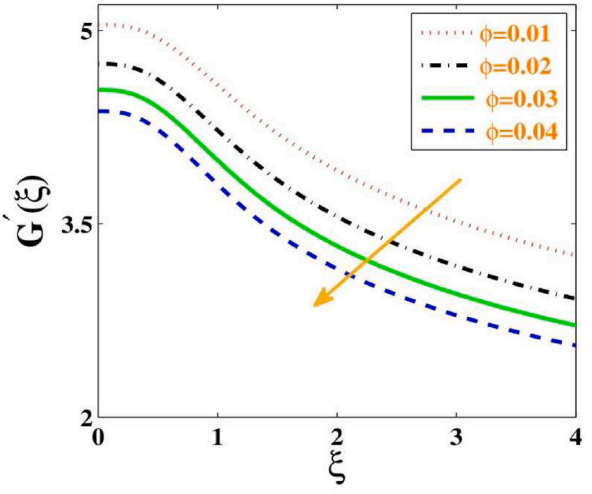

Fig. 3. $G^{'}(\xi)$ Change withφ.

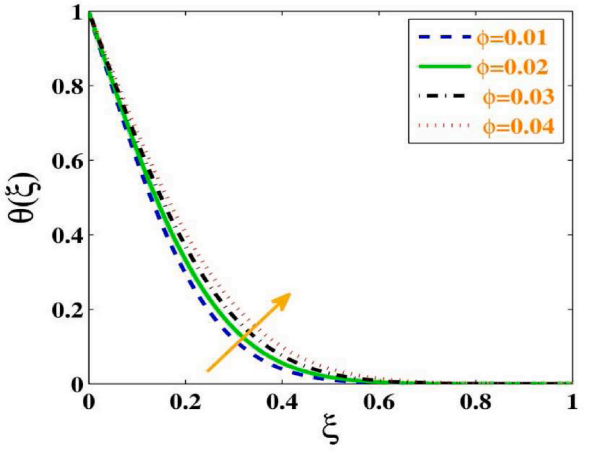

Fig. 4. $\theta(\xi)$ Change with φ.

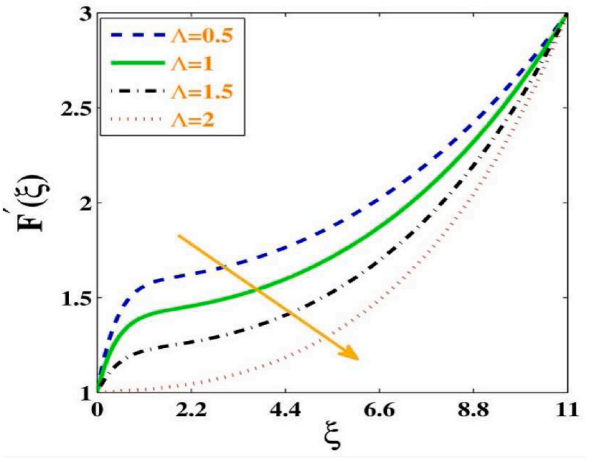

Fig. 5. Velocity alteration with Λ.

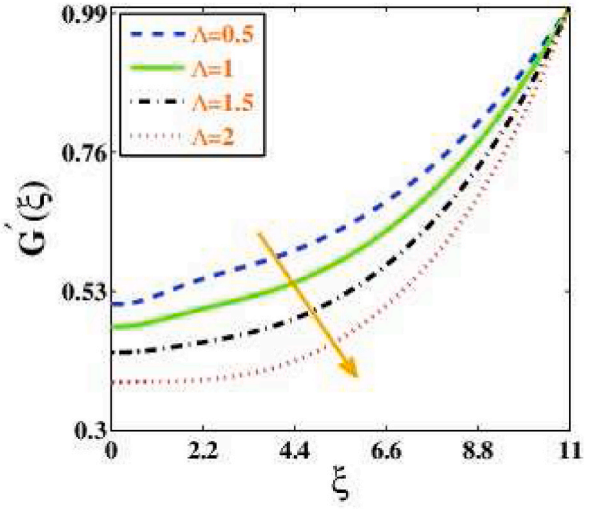

Fig. 6. $G^{'}(\xi)$ Alteration with Λ.

wefts on stretch sheets. The following considerations are based on the Keller-boxnumeric scheme's calculated numerical and graph results.This phase affords the results of bodily parameters specifically A^{*}, φ, Λ, λ^{*}, Q_0 ,N_r, P_r, ε, R_e and B_r. Moving influence of fluid's velocity, temperature and entropy generation are represented in Figs. 2–8. The conclusions are made for Ti_6Al_4V– H_2O based Newtonian nanofluid. We done this numerical analysis by conveying altered values to changed parameters (i.e., $A^{*} = 0.6$, $\varphi = 0.01$, $\Lambda = 0.5$, $Q_0 = 0.5$, $\lambda^{*} = 0.6$,$N_r = 0.2$, $P_r = 6.2$, $\varepsilon = 0.1$, $R_e = 5$ and $B_r = 5$).

7.1. Effect of nanoparticle volume fraction (φ)

Figs. 2–4 depict the consequence of nanoparticle volume fraction on nanofluid velocity, entropy, and temperature contours, individually. The velocity field of a nanofluid subjected to a volumetric proportion of nanoparticles is depicted in Fig. 2. When the volume fraction is increased, the velocity of the nanofluid appears to diminution. Fig. 3 depicts the consequence of nanoparticle volume fraction on nanofluid entropy profile. $G^{'}(\xi)$. A progressive increase in volumetric fraction is reflected as a dip in the entropy profile. Figs. 2 and 3 explains that the rate and magnetic discipline profiles cut back because of extent faction of nanoparticles in each effects and so impede the rate and magnetic parameter boundary-layers. Physically, the nanoparticle extent fractions delivered in flourishing viscosity of a convectional everyday fluid, i.e., water withinside the modern-day investigation. Fig. four depicts the variant in temperature discipline proportional to the extent fraction of nanoparticles. It became found that growing the extent fraction price ended in a growth temperature withinside the fluid. In essence, the temperature of the sheet is amplified because the mass of the nanoparticles enlarges, as a result the performance of thermal conductivity decreases and therefore influences the warmth switch charge of the operating fluid. This may also arise as a result of the inner warmness technology impacts that improved the temperature during the floor and disrupted the interplay of the nanoparticles, which then lower the thermal conductivities. Accordingly, the

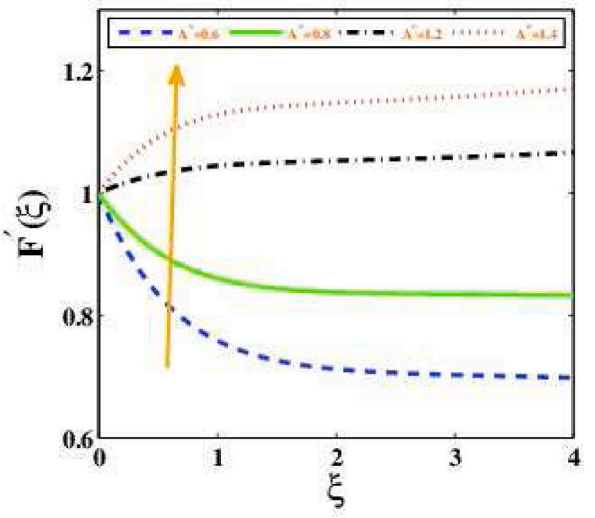

Fig. 7. Velocity change with A^*.

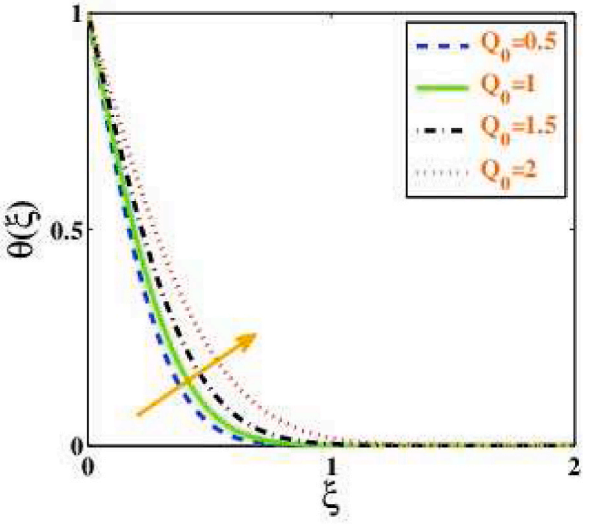

Fig. 8. $\theta(\xi)$ change with Q_0.

modern-day findings display that the usage of nanomaterials can assist us expand stepped forward warmness movement specially warmness switch gadget and might gather electricity thru chemical processes.

7.2. *Influence of magnetic parameter (Λ)*

The change in velocity field of nanofluid subject to magnetic parameter is illustrated in Figs. 5 and 6, which show the variation in velocityand entropy fields with regard to magnetic field. When the value of the magnetic field parameter is improved, the velocity field of the nanofluid drops. The parametric impact of magnetic field on nanofluid entropy profile $G^{'}(\xi)$ is shown in Fig. 6. With a gradual increase in magnetic field, the profile of entropy creation $G^{'}(\xi)$ decreases.In Figs. 5 and 6, $F^{'}(\xi)$ and $G^{'}(\xi)$ decrease as M increasesdue to the opposite pressure, particularly Lorentz pressure. This pressure seems to decrease the fluid pace because of resistance in opposition to the movement of the fluid particles. The synchronisation of an electrical and magnetic subject springing up as a result of the advent of Lorentz pressure seems to postpone fluid progress.

7.3. *Influence of stretching parameter (A^*)*

Modification in velocity, temperature, and entropy fields with respect to stretching parameter A^* is showed in Fig. 7. Fig. 7 is representing the change in velocity field of nanofluid subjected to stretching parameter A^*. When A^* <1, collective behavior is observed in velocity field of nanofluid. Same phenomenon occurs when $A^* > 1$. Furthermore, it is observed that overall fluid flow rises

Table 4

Standards of skin friction $= C_f Re_x^{\frac{1}{2}}$ and Nusselt number $= Nu_x Re_x^{\frac{-1}{2}}$ for $P_r = 6.2$.

A^*	Λ	φ	λ^*	Q_0	Nr	ε	$C_f Re_x^{\frac{1}{2}}$	$N_u Re_x^{\frac{-1}{2}}$ Basefluid	$N_u Re_x^{\frac{-1}{2}}$ Nanofluid
0.6	0.5	0.01	0.6	0.5	0.2	0.1	0.6186	8.1187	9.5193
0.8							0.5346	8.1364	9.5378
1.2							0.4502	8.1540	9.5831
	0.5						0.6186	8.1187	9.5193
	1						0.5910	8.1581	9.5477
	1.5						0.5703	8.1958	9.5650
		0.01					0.6186	8.1187	9.5193
		0.02					0.6425	8.1650	9.6248
		0.03					0.6681	8.2121	9.6505
			0.6				0.6186	8.1187	9.5193
			0.8				0.6564	8.0897	9.4830
			1.0				0.6738	8.0657	9.4673
				0.5			0.6186	8.1187	9.5193
				1			0.6186	8.1557	9.5510
				1.5			0.6186	8.1955	9.5852
					0.1		0.6186	8.0870	9.4356
					0.2		0.6186	8.1187	9.5193
					0.3		0.6186	8.1487	9.5441
						0.1	0.6186	8.1187	9.5193
						0.2	0.6186	8.0702	9.4794
						0.3	0.6186	8.0497	9.4587

with the rise in stretching parameter.

7.4. Influence of heat source/sink parameter (Q_0)

Fig. 8 illustrate the influence of heat source or sink parameter Q_0 on the temperature profiles of the flow. It is clear that an increase in the non-uniform heat source or sink parameter enhances the temperature profiles of the flow, this hike in temperature profiles is more significant in radiation case. Generally, positive values of Q_0, are acts like heat generators. Generating the heat means releasing the heat energy to the flow, these causes to develop the temperature profiles of the flow.

7.5. Heat transfer rate in (Ti_6Al_4V– H_2O) nanofluid

For a static use of nanoparticles, the thermodynamic effects of Titanium alloy (Ti_6Al_4V) based water (H_2O) nanofluid are observed. The thermal conductivity of a fluid increases as its temperature rises. Ti_6Al_4V has a higher thermal conductivity than H_2O, making it a good platform for nanofluid heat transfer. This operation is recommended for applications that require a lot of heat transmission. The relative Nusselt number Nu_x calculated for various physical factors indicates this fact. Table 4 has the results for your readers to use.

8. Closing remarks

The idea of the cutting-edge evaluate is to analyze the exhibition of heat framework in the sight of a development of Induced MHD nanofluids streaming overextend foil. A few sizable discoveries from the exam are:

Temperature profile will increase for nanoparticles extent fraction, magnetic subject parameter, Q_0, N_r, ε in addition to reciprocal of magnetic Prandtl range. Meanwhile deceleration in fluid temperature is received for stretching parameter in addition to Prandtl range. Velocity subject of nanofluid decreases for volumetric fraction of nanoparticles, magnetic parameter in addition to reciprocal of magnetic Prandtl range. However, increment is received for stretching parameter.Increment in entropy subject of nanofluid is received for Reynolds range as well as Brinkman range however discount is received for stretching parameter, volumetric fraction of nanoparticles, magnetic subject parameter and reciprocal of magnetic Prandtl range.

8.1. Future orientation

When considerations are made on more physical surroundings and remaining industrial difficulties that need to be solved, numerous hybrid nanofluid combos can be produced in the future to achieve heat transmission rates for linked challenges. The Keller-box method could be applied to a variety of physical and technical challenges in the future [82–96].

Credit author statement

Conceptualization: Wasim Jamshed, Formal analysis: Faisal Shahzad, Investigation: Wasim Jamshed & Rabia Safdar, Methodology: Wasim Jamshed & Misbah Arshad, Software: Faisal Shahzad & Syed M. Hussain, Writing - original draft: Faisal Shahzad, Wasim Jamshed & Rabia Safdar, Writing - review editing: Syed M. Hussain, Amjad Ali Pasha & Misbah Arshad, Validation: Amjad Ali Pasha, Muhammad Bilal Hafeez, Marek Krawczuk, & Md. MottahirAlam.

Declaration of competing interest

The authors declare that they have no known competing financial interests or personal relationships that could have appeared to influence the work reported in this paper.

Acknowledgment

This project was funded by the Deanship of Scientific Research (DSR), King Abdulaziz University, Jeddah, under grant No. (D-734-135-1443). The authors, therefore, gratefully acknowledge DSR technical and financial support.

References

[1] T.L. Bergman, A.S. Lavine, F.P. Incropera, D.P. DeWitt, Introduction to Heat Transfer, John Wiley & Sons, 2011.
[2] J. Serrano, P. Olmeda, F. Arnau, M. Reyes-Belmonte, A. Lefebvre, Importance of heat transfer phenomena in small turbochargers for passenger car applications, SAE Intern. J. Engines. 6 (2) (2013) 716–728.
[3] H. Zhang, J. Zhuang, Research, development and industrial application of heat pipe technology in China, Appl. Therm. Eng. 23 (9) (2003) 1067–1083.
[4] K.N. Ramesh, T.K. Sharma, G. Rao, Latest advancements in heat transfer enhancement in the micro-channel heat sinks: a review, Arch. Comput. Methods Eng. 28 (4) (2021) 3135–3165.
[5] L.A. Pozhar, Structure and dynamics of nanofluids: theory and simulations to calculate viscosity, Phys. Rev. 61 (2) (2000) 1432.
[6] M. Rafati, A. Hamidi, M.S. Niaser, Application of nanofluids in computer cooling systems (heat transfer performance of nanofluids), Appl. Therm. Eng. 45 (2012) 9–14.
[7] G. Polidori, S. Fohanno, C. Nguyen, A note on heat transfer modelling of Newtonian nanofluids in laminar free convection, Int. J. Therm. Sci. 46 (8) (2007) 739–744.
[8] G. Huminic, A. Huminic, Application of nanofluids in heat exchangers: a review, Renew. Sustain. Energy Rev. 16 (8) (2012) 5625–5638.
[9] H. Schlichting, K. Gersten, Boundary-layer Theory, Springer Science & Business Media, 2003.
[10] V.M. Luchesi, R.T. Coelho, An inverse method to estimate the moving heat source in machining process, Appl. Therm. Eng. 45 (2012) 64–78.
[11] H.-C. Tran, Y.-L. Lo, Heat transfer simulations of selective laser melting process based on volumetric heat source with powder size consideration, J. Mater. Process. Technol. 255 (2018) 411–425.
[12] Y.S. Muzychka, Influence coefficient method for calculating discrete heat source temperature on finite convectively cooled substrates, IEEE Trans. Compon. Packag. Technol. 29 (3) (2006) 636–643.
[13] B.K. Jha, S. Isa, Computational treatment of MHD transient natural convection flow in a vertical channel due to symmetric heating in presence of induced magnetic field, J. Phys. Soc. Jpn. 82 (8) (2013), 084401.
[14] A. Kumar, A. Singh, Unsteady MHD free convective flow past a semi-infinite vertical wall with induced magnetic field, Appl. Math. Comput. 222 (2013) 462–471.
[15] R.K. Singh, A.K. Singh, N.C. Sacheti, P. Chandran, On hydromagnetic free convection in the presence of induced magnetic field, Heat Mass Tran. 46 (5) (2010) 523–529.
[16] S. Ghosh, O. Anwar Bég, J. Zueco, Hydromagnetic free convection flow with induced magnetic field effects, Meccanica 45 (2) (2010) 175–185.
[17] A. Singh, Magnetohydrodynamic free convection between vertical parallel porous plates in the presence of induced magnetic field, SpringerPlus 4 (1) (2015) 1–13.
[18] J. Kwanza, J. Balakiyema, Magnetohydrodynamic free convective flow past an infinite vertical porous plate with magnetic induction, J. Fusion Energy 31 (4) (2012) 352–356.
[19] N.S. Akbar, M. Raza, R. Ellahi, Interaction of nanoparticles for the peristaltic flow in an asymmetric channel with the induced magnetic field, Eur. Phys. J. Plus. 129 (7) (2014) 1–12.
[20] N.S. Akbar, M. Raza, R. Ellahi, Influence of induced magnetic field and heat flux with the suspension of carbon nanotubes for the peristaltic flow in a permeable channel, J. Magn. Magn Mater. 381 (2015) 405–415.
[21] S. Ahmed, J. Zueco, L.M. López-González, Effects of chemical reaction, heat and mass transfer and viscous dissipation over a MHD flow in a vertical porous wall using perturbation method, Int. J. Heat Mass Tran. 104 (2017) 409–418.
[22] B.K. Jha, B. Aina, Role of induced magnetic field on MHD natural convection flow in vertical microchannel formed by two electrically non-conducting infinite vertical parallel plates, Alex. Eng. J. 55 (3) (2016) 2087–2097.
[23] S. Rostami, D. Toghraie, B. Shabani, N. Sina, P. Barnoon, Measurement of the thermal conductivity of MWCNT-CuO/water hybrid nanofluid using artificial neural networks (ANNs), J. Therm. Anal. Calorim. 143 (2) (2021) 1097–1105.
[24] A.R. Rahmati, O.A. Akbari, A. Marzban, D. Toghraie, R. Karimi, F. Pourfattah, Simultaneous investigations the effects of non-Newtonian nanofluid flow in different volume fractions of solid nanoparticles with slip and no-slip boundary conditions, Therm. Sci. Eng. Prog. 5 (2018) 263–277.
[25] S. Oveissi, D. Toghraie, S.A. Eftekhari, Longitudinal vibration and stability analysis of carbon nanotubes conveying viscous fluid, Phys. E Low-dimens. Syst. Nanostruct. 83 (2016) 275–283.
[26] M. Tohidi, D. Toghraie, The effect of geometrical parameters, roughness and the number of nanoparticles on the self-diffusion coefficient in Couette flow in a nanochannel by using of molecular dynamics simulation, Phys. B Condens. Matter 518 (2017) 20–32.
[27] H. Kavusi, D. Toghraie, A comprehensive study of the performance of a heat pipe by using of various nanofluids, Adv. Powder Technol. 28 (11) (2017) 3074–3084.
[28] A. Moraveji, D. Toghraie, Computational fluid dynamics simulation of heat transfer and fluid flow characteristics in a vortex tube by considering the various parameters, Int. J. Heat Mass Tran. 113 (2017) 432–443.
[29] Z. Li, P. Barnoon, D. Toghraie, R.B. Dehkordi, M. Afrand, Mixed convection of non-Newtonian nanofluid in an H-shaped cavity with cooler and heater cylinders filled by a porous material: two phase approach, Adv. Powder Technol. 30 (11) (2019) 2666–2685.
[30] B. Ruhani, P. Barnoon, D. Toghraie, Statistical investigation for developing a new model for rheological behavior of Silica–ethylene glycol/Water hybrid Newtonian nanofluid using experimental data, Phys. Stat. Mech. Appl. 525 (2019) 616–627.
[31] A. Young, Aerodynamics. By L. J. CLANCY. Pitman, 1975. 610 pp.£ 10.00, J. Fluid Mech. 77 (3) (1976) 623–624.
[32] R.W. Fox, A.T. McDonald, J.W. Mitchell, Fox and McDonald's Introduction to Fluid Mechanics, John Wiley & Sons, 2020.
[33] J.D. Anderson, McGraw-Hill Series in Aeronautical and Aerospace Engineering, Fundamentals of Aerodynamics, 2003, pp. 54–56.
[34] H.T. Phan, N. Caney, P. Marty, S. Colasson, J. Gavillet, Surface wettability control by nanocoating: the effects on pool boiling heat transfer and nucleation mechanism, Int. J. Heat Mass Tran. 52 (23–24) (2009) 5459–5471.
[35] M.E. Burnett, S.Q. Wang, Current sunscreen controversies: a critical review, Photodermatol. Photoimmunol. Photomed. 27 (2) (2011) 58–67.
[36] D. Lapotko, Plasmonic nanoparticle-generated photothermal bubbles and their biomedical applications, Nanomedicine 4 (7) (2009) 813–845.
[37] K. Maier-Hauff, R. Rothe, R. Scholz, Intracranial thermotherapy using magnetic nanoparticles combined with external beam radiotherapy: results of a feasibility study on patients with glioblastoma multiforme, J. Neuro Oncol. 81 (1) (2007) 53–60.
[38] D.P. Kulkarni, D.K. Das, R.S. Vajjha, Application of nanofluids in heating buildings and reducing pollution, Appl. Energy 86 (12) (2009) 2566–2573.
[39] L. Vékás, D. Bica, M.V. Avdeev, Magnetic nanoparticles and concentrated magnetic nanofluids: synthesis, properties and some applications, China Particuol. 5 (1–2) (2007) 43–49.

[40] T. Sharma, A.L.M. Reddy, T.S. Chandra, S. Ramaprabhu, Development of carbon nanotubes and nanofluids based microbial fuel cell, Int. J. Hydrogen Energy 33 (22) (2008) 6749–6754.
[41] R. Taylor, S. Coulombe, T. Otanicar, et al., Small particles, big impacts: a review of the diverse applications of nanofluids, J. Appl. Phys. 113 (1) (2013). Article ID 011301.
[42] Scopus-Database, Nanofluids Analyze Search Results from 2015 to 2018, Elsevier, 2018.
[43] S. Singh, D. Kumar, K.N. Rai, Convective-radiative fin with temperature dependent thermal conductivity, heat transfer coefficient and wavelength dependent surface emissivity, Propuls. Power. Res. 3 (4) (2014) 207–221.
[44] A.S.V. Ravikanth, U.K. Niyan, A haar wavelet study on convective-radiative fin under continuous motion with temperature-dependent thermal conductivity, Walailak J. Sci. Technol. 11 (3) (2014) 211–224.
[45] A.S. Dogonchi, D.D. Ganji, Convection–radiation heat transfer study of moving fin with temperature-dependent thermal conductivity, heat transfer coefficient and heat generation, Appl. Therm. Eng. 103 (2016) 705–712.
[46] T.-H. Park, N.-W. Park, J. Kim, W.-Y. Lee, J.-H. Koh, S.-K. Lee, Cross-plane temperature-dependent thermal conductivity of Al-doped zinc oxide thin films, J. Alloys Compd. 638 (2015) 83–87.
[47] W. Pan, F. Yi, Y. Zhu, S. Meng, Identification of temperature-dependent thermal conductivity and experimental verification, Meas. Sci. Technol. 27 (7) (2016). Article ID 075005.
[48] M.I.A. Othman, R.S. Tantawi, E.E.M. Eraki, Effect of initial stress on a semiconductor material with temperature dependent properties under DPL model, Microsyst. Technol. 23 (12) (2017) 5587–5598.
[49] A.M. Zenkour, A.E. Abouelregal, Nonlocal thermoelastic nanobeam subjected to a sinusoidal pulse heating and temperature-dependent physical properties, Microsyst. Technol. 21 (8) (2015) 1767–1776.
[50] C. Xiong, Y. Guo, Effect of variable properties and moving heat source on magnetothermoelastic problem under fractional order thermoelasticity, Adv. Mater. Sci. Eng. 2016 (2016). Article ID 5341569, 12 pages.
[51] Y. Wang, D. Liu, Q. Wang, J. Zhou, Asymptotic solutions for generalized thermoelasticity with variable thermal material properties, Arch. Mech. 68 (3) (2016) 181–202.
[52] M.A. Ezzat, A.A. El-Bary, On thermo-viscoelastic infinitely long hollow cylinder with variable thermal conductivity, Microsyst. Technol. 23 (8) (2017) 3263–3270.
[53] S.M. Abo-Dahab, I.A. Abbas, LS model on thermal shock problem of generalized magneto-thermoelasticity for an infinitely long annular cylinder with variable thermal conductivity, Appl. Math. Model. 35 (8) (2011) 3759–3768.
[54] C. Li, H. Guo, X. Tian, X. Tian, Transient response for a half-space with variable thermal conductivity and diffusivity under thermal and chemical shock, J. Therm. Stresses 40 (3) (2016) 389–401.
[55] K. Ramesh, M. Devakar, Influence of heat transfer on the peristaltic transport of Walters B fluid in an inclined annulus, J. Braz. Soc. Mech. Sci. Eng. 39 (7) (2017) 2571–2584.
[56] K. Ramesh, M. Gnaneswara Reddy, M. Devakar, Biomechanical study of magnetohydrodynamic Prandtl nanofluid in a physiological vessel with thermal radiation and chemical reaction, Proc. Inst. Mech. Eng., Part N: Journal of Nanomaterials, Nanoengineering and Nanosystems 232 (4) (2018) 95–108.
[57] K. Ramesh, M. Devakar, Peristaltic transport of MHD Williamson fluid in an inclined asymmetric channel through porous medium with heat transfer, J. Cent. S. Univ. 22 (8) (2015) 3189–3201.
[58] K. Ramesh, M. Reddy, B. Souayeh, Electro-magneto-hydrodynamic flow of couple stress nanofluids in micro-peristaltic channel with slip and convective conditions, Appl. Math. Mech. 42 (4) (2021) 593–606.
[59] R. Katta, P. Jayavel, Heat transfer enhancement in radiative peristaltic propulsion of nanofluid in the presence of induced magnetic field, Numer. Heat Tran., Part A: Applications 79 (2) (2020) 83–110.
[60] K. Ramesh, S.A. Eytoo, Effects of thermal radiation and magnetohydrodynamics on Ree-Eyring fluid flows through porous medium with slip boundary conditions, Multidiscip. Model. Mater. Struct. (2018).
[61] K. Ramesh, M. Devakar, Influence of magnetohydrodynamics on peristaltic flow of a Walters B fluid in an inclined asymmetric channel with heat transfer, World J. Eng. (2018).
[62] B. Gireesha, B. Mahanthesh, I. Shivakumara, K. Eshwarappa, Melting heat transfer in boundary layer stagnation-point flow of nanofluid toward a stretching sheet with induced magnetic field, Eng. Sci. Technol, Intern. J. 19 (1) (2016) 313–321.
[63] D. Makinde, B. Mahanthesh, B.J. Gireesha, N. Shashikumar, R. Monaledi, M. Tshehla, MHD nanofluid flow past a rotating disk with thermal radiation in the presence of aluminum and titanium alloy nanoparticles, Defect Diffusion Forum 384 (2018) 69–79. Trans Tech Publ.
[64] W. Jamshed, K.S. Nisar, R.W. Ibrahim, T. Mukhtar, V. Vijayakumar, F. Ahmad, Computational frame work of Cattaneo-Christov heat flux effects on Engine Oil based Williamson hybrid nanofluids: a thermal case study, Case Stud. Therm. Eng. 26 (2021), 101179.
[65] Z. Iqbal, E. Azhar, Z. Mehmood, E. Maraj, A. Kamran, Computational analysis of engine-oil based magnetite nanofludic problem inspired with entropy generation, J. Mol. Liq. 230 (2017) 295–304.
[66] N.B. Reddy, T. Poornima, P. Sreenivasulu, Influence of variable thermal conductivity on MHD boundary layer slip flow of ethylene-glycol based Cu nanofluids over a stretching sheet with convective boundary condition, Int. J Eng. Math. 2014 (2014), 905158.
[67] W. Jamshed, S.U. Devi S, M. Goodarzi, M. Prakash, K.S. Nisar, M. Zakarya, A.H. Abdel-Aty, Evaluating the unsteady Casson nanofluid over a stretching sheet with solar thermal radiation: an optimal case study, Case Stud. Therm. Eng. 26 (2021), 101160.
[68] W. Jamshed, S.R. Mishra, P.K. Pattnaik, K.S. Nisar, S.S.U. Devi, M. Prakash, F. Shahzad, M. Hussain, V. Vijayakumar, Features of entropy optimization on viscous second grade nanofluid streamed with thermal radiation: a Tiwari and Das model, Case Stud. Therm. Eng. 27 (2021), 101291.
[69] W. Jamshed, M.R. Eid, N.A.A. Mohd Nasir, K.S. Nisar, A. Aziz, F. Shahzad, C.A. Saleel, A. Shukla, Thermal examination of renewable solar energy in parabolic trough solar collector utilizing Maxwell nanofluid: a noble case study, Case Stud. Therm. Eng. 27 (2021), 101258.
[70] W. Jamshed, K.S. Nisar, S.S.P. Mohamed Isa, S. Batool, A.H. Abdel-Aty, M. Zakarya, Computational case study on tangent hyperbolic hybrid nanofluid flow: single phase thermal investigation, Case Stud. Therm. Eng. 27 (2021), 101246.
[71] W. Jamshed, S.U. Devi S, M. Goodarzi, M. Prakash, K.S. Nisar, M. Zakarya, A.H. Abdel-Aty, Evaluating the unsteady Casson nanofluid over a stretching sheet with solar thermal radiation: an optimal case study, Case Stud. Therm. Eng. 26 (2021), 101160.
[72] W. Jamshed, A. Aziz, A comparative entropy based analysis of Cu and Fe_3O_4/methanol Powell-Eyring nanofluid in solar thermal collectors subjected to thermal radiation, variable thermal conductivity and impact of different nanoparticles shape, Results Phys. 9 (2018) 195–205.
[73] W. Jamshed, et al., A brief comparative examination of tangent hyperbolic hybrid nanofluid through an extending surface: numerical Keller–Box scheme, Sci. Rep. 11 (1) (2021) 1–32.
[74] F. Ahmad, S. Abdal, H. Ayed, S. Hussain, S. Salim, A.O. Almatroud, The improved thermal efficiency of Maxwell hybrid nanofluid comprising of graphene oxide plus silver/kerosene oil over stretching sheet, Case Stud. Therm. Eng. 27 (2021), 101257.
[75] W. Jamshed, Numerical investigation of MHD impact on Maxwell nanofluid, Int. Commun. Heat Mass Tran. 120 (2021), 104973.
[76] M.Q. Brewster, Thermal Radiative Transfer and Properties, John Wiley & Sons, 1992.
[77] H.B. Keller, A new difference scheme for parabolic problems, in: Numerical Solution of Partial Differential Equations–II, Elsevier, 1971, pp. 327–350.
[78] W. Jamshed, A. Aziz, Entropy analysis of TiO_2-Cu/EG casson hybrid nanofluid via Cattaneo-Christov heat flux model, Appl. Nanosci. (2018) vol. 08, pp. 01–14.
[79] W. Jamshed, K.S. Nisar, Computational single-phase comparative study of a Williamson nanofluid in a parabolic trough solar collector via the Keller box method, Int. J. Energy Res. 45 (7) (2021) 10696–10718.
[80] S. Das, S. Chakraborty, R. Jana, O. Makinde, Entropy analysis of unsteady magneto-nanofluid flow past accelerating stretching sheet with convective boundary condition, Appl. Math. Mech. 36 (12) (2015) 1593–1610.
[81] S.M. Hussain, Thermal-enhanced hybrid of copper–zirconium dioxide/ethylene glycol nanofluid flowing in the solar collector of water-pump application, Waves Random Complex Media (2022) 1–28.

[82] T.-H. Zhao, Z.-Y. He, Y.-M. Chu, Sharp bounds for the weighted Hölder mean of the zero-balanced generalized complete elliptic integrals, Comput. Methods Funct. Theor. 21 (3) (2021) 413–426.
[83] T.-H. Zhao, W.-M. Qian, Y.-M. Chu, Sharp power mean bounds for the tangent and hyperbolic sine means, J. Math. Inequalities 15 (4) (2021) 1459–1472.
[84] Y.-M. Chu, U. Nazir, M. Sohail, M.M. Selim, J.-R. Lee, Enhancement in thermal energy and solute particles using hybrid nanoparticles by engaging activation energy and chemical reaction over a parabolic surface via finite element approach, Fractal. Fract. 5 (3) (2021) 119.
[85] M.D. Ikram, M.A. Imran, Y.M. Chu, A. Akgül, MHD flow of a Newtonian fluid in symmetric channel with ABC fractional model containing hybrid nanoparticles, Comb. Chem. High Throughput Screen. 25 (7) (2022) 1087–1102.
[86] S. Rashid, S. Sultana, Y. Karaca, A. Khalid, Y.-M. Chu, Some further extensions considering discrete proportional fractional operators, Fract. 30 (2022), 2240026, 01.
[87] a F. Jin, Z.-S. Qian, Y.-M. Chu, M. ur Rahman, On nonlinear evolution model for drinking behavior under Caputo-Fabrizio derivative, J. Appl. Anal. Comput. 12 (2) (2022) 790–806;
b Y.M. Chu, S. Bashir, M. Ramzan, M.Y. Malik, Model-based comparative study of magnetohydrodynamics unsteady hybrid nanofluid flow between two infinite parallel plates with particle shape effects, Math. Methods Appl. Sci. (2022).
[88] F. Wang, M.N. Khan, I. Ahmad, H. Ahmad, H. Abu-Zinadah, Y.-M. Chu, Numerical solution of traveling waves in chemical kinetics: time-fractional Fishers equations, Fract. 30 (2022), 2240051, 02.
[89] M. Nazeer, F. Hussain, M.I. Khan, E.R. El-Zahar, Y.-M. Chu, M. Malik, Theoretical study of MHD electro-osmotically flow of third-grade fluid in micro channel, Appl. Math. Comput. 420 (2022), 126868.
[90] Y.-M. Chu, B. Shankaralingappa, B. Gireesha, F. Alzahrani, M.I. Khan, S.U. Khan, Combined impact of Cattaneo-Christov double diffusion and radiative heat flux on bio-convective flow of Maxwell liquid configured by a stretched nano-material surface, Appl. Math. Comput. 419 (2022), 126883.
[91] I. Ullah, Heat transfer enhancement in Marangoni convection and nonlinear radiative flow of gasoline oil conveying Boehmite alumina and aluminum alloy nanoparticles, Int. Commun. Heat Mass Tran. 132 (2022), 105920.
[92] I. Ullah, Activation energy with exothermic/endothermic reaction and Coriolis force effects on magnetized nanomaterials flow through Darcy–Forchheimer porous space with variable features, Waves Random Complex Media (2022) 1–14.
[93] K. Ali, S. Ahmad, O. Baluch, W. Jamshed, M.R. Eid, A.A. Pasha, Numerical study of magnetic field interaction with fully developed flow in a vertical duct, Alex. Eng. J. 61 (2022) 11351–11363.
[94] K. Ali, A.A. Faridi, S. Ahmad, W. Jamshed, N. Khan, M.M. Alam, Quasi-linearization analysis for heat and mass transfer of magnetically driven 3rd-grade (Cu-TiO_2/engine oil) nanofluid via a convectively heated surface, Int. Commun. Heat Mass Tran. 135 (2022), 106060.
[95] W. Jamshed, M.R. Eid, S.M. Hussain, A. Abderrahmane, R. Safdar, O. Younis, A.A. Pasha, Physical specifications of MHD mixed convective of Ostwald-de Waele nanofluids in a vented-cavity with inner elliptic cylinder, Int. Commun. Heat Mass Tran. 134 (2022), 106038.
[96] M.B. Hafeez, M. Krawczuk, K.S. Nisar, W. Jamshed, A.A. Pasha, A finite element analysis of thermal energy inclination based on ternary hybrid nanoparticles influenced by induced magnetic field, Int. Commun. Heat Mass Tran. 135 (2022), 106074.